Redefining the Mobility Edge in Thin-Film Transistors

Xiao Wang,[1,2] Leonard F. Register,[1,2] and Ananth Dodabalapur[1,2,*]

[1]*Department of Electrical and Computer Engineering, The University of Texas at Austin, Austin, Texas 78712, USA*
[2]*Microelectronics Research Center, The University of Texas at Austin, Austin, Texas 78758, USA*

In most thin-film transistors, the concept of mobility edge needs to be redefined to take into account important constraints. We describe how the mobility edge concept has to be reinterpreted when applied to thin-film transistors. Charge carriers can be significantly localized due to strong scattering, altering the model of band transport in extended states so that, effectively, only a fraction of carriers can actually move in the extended states, in accordance with a statistical distribution of free paths. It is necessary to explicitly consider this effect in applying conventional semiconductor transport theories based on solutions to the Boltzmann transport equation (BTE). We are then able to apply the BTE with appropriate scattering mechanisms and obtain results that agree well with experiment for the case of a polymer thin-film transistor (TFT). This approach is very well suited to thin-film transistors based on polymer and organic semiconductors, and also many amorphous oxide semiconductors with room temperature mobilities in the range 1–20 cm^2/(Vs).

I. INTRODUCTION

For band transport or extended state transport to take place in a semiconductor, it is commonly believed that the mean free path must be much greater than the lattice constant. The mean free path can be considered to be the average distance charge carriers travel between scattering events. When carrier mobilities are more than about 20 cm^2/(Vs), the mean free paths exceed typical lattice constants and intermolecular distances [1,2]. At these mobility values and beyond, charge transport theories based on the Boltzmann transport equation (BTE) can be applied. This approach has been used successfully for several semiconductors such as Si and GaAs [3,4]. For semiconductors with a high density of localized trap states, carriers can become bound to these states and no longer contribute to transport except by hopping. The "mobility edge" is an elegant principle that has been applied to many semiconductor systems [5–7] and is normally understood to be the energy that separates localized trap states from extended states [6,7]. However, for semiconductors possessing very small mean free paths, even application of conventional band transport theory within nominally extended states above the mobility edge energy is problematic, and hoppinglike transport of localized carriers dominates. This transition from band to hoppinglike transport occurs when the mean free path is comparable to the intermolecular distances or lattice constants, typically about

*ananth.dodabalapur@engr.utexas.edu

0.3 nm. Many thin-film transistors (TFTs) have mobilities in the range of 1–20 cm^2/(Vs) [8–27], which corresponds to mean free paths that are of the order of 0.3 nm.

Figure 1 is a schematic plot of path length versus energy in TFTs. The mobility edge is also indicated in the figure. These path lengths are described with reference to the lattice constant, *a*. For large path lengths, which are much more than the lattice constant (i.e., in high mobility semiconductors), the mobility edge separates the localized states from the delocalized states. This is in accordance with the pioneering analysis by Mott [6,7]. When the path lengths are smaller (of order *a*), the mobility edge still separates the localized states from the delocalized states; however, many of the carriers in delocalized states may become effectively localized by strong scattering. For even smaller path length ($\ll a$), all states are localized and only hopping transport between localized states is possible. This type of behavior is seen in many amorphous organic semiconductors [28,29]. It is for the intermediate path length semiconductors that conventional transport theories have proven to be difficult to apply. To solve the problem, we hypothesize that some of the carriers above the mobility edge are effectively localized by strong scattering and only a fraction of carriers above the mobility edge contribute to current resulting from band transport. Carriers above the mobility edge that are effectively localized, however, do contribute to screening of Coulomb potentials. In Fig. 2, the different types of charge carriers are represented schematically as a function of carrier density. Our definition of mobility edge is, therefore, different from
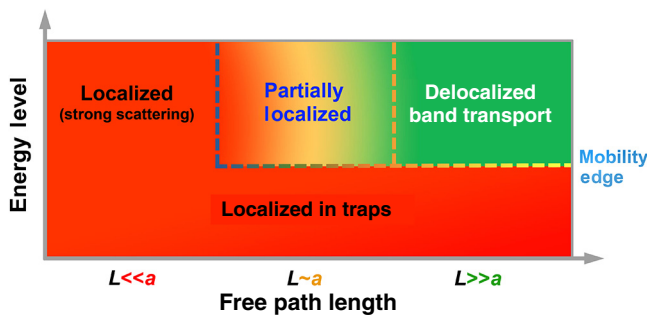
FIG. 1. Schematic plot of charge localization vrsues energy and free path length within extended states. The mobility edge separates the carriers into two broad categories: localized carriers, consistent with the traditional definition of mobility edge, below the mobility edge, and carriers above the mobility edge. Above the mobility edge, when the carrier free path is much smaller than the lattice constant and/or intermolecular distance a, however, band transport remains unlikely. When the free path is much larger than a, conventional band transport calculations are possible. When the mean free path is between these limits, not all carriers that are excited above the mobility edge are able to move by means of band transport. In such cases, there is a fraction of carriers that are effectively localized due to strong scattering. These effectively localized carriers, however, can still contribute to screening and can move by hopping.

the original definition based on Mott in which all carriers above the mobility edge move in extended states [6]. The statistical distribution of path lengths and the calculation of the fraction of carriers actually involved in band transport becomes important. We propose the use of a transport reduction factor (P_{TRF}) to scale calculations to take account of the carriers above the mobility edge that are still effectively localized by strong scattering. In the following section, we describe the P_{TRF} concept after first outlining the BTE and its solution as applied to semiconductor mobility calculations relevant to this work.

The method of analysis we describe in this paper may not be applicable in the case of very narrow bandwidth semiconductors or semiconductors in which polaron theory applies. In Section II we use the criterion proposed by Kenkre et al. [30] to establish the range of validity of our analysis procedure.

II. CALCULATION PROCEDURE FOR MOBILITY IN THIN-FILM TRANSISTORS

The BTE has been used as the basis to calculate mobilities in various inorganic semiconductors such as Si and GaAs [3,4]. In many cases, solutions based on the relaxation time approximation (RTA) are used. Moreover, while scattering is neither local in position nor instantaneous, and transport and scattering occur simultaneously, the picture of free flights separated by instantaneous scattering events remains a mathematically valid approach to address the

BTE (as per the example of semiclassical Monte Carlo). As noted in the introduction, an essential prerequisite for the use of the BTE is that the mean free path between scattering events be greater than the lattice constant, a condition easily met in many semiconductors. In the case of disordered semiconductors such as polymers and amorphous oxides, however, this condition is not generally satisfied. Only in a few instances with relatively high mobilities [1] can the RTA be used. In most other cases, the mean free path is equal to or slightly less than the lattice constant or intermolecular distance. This limited mean free path has been an obstacle in the using the BTE to analyze charge transport in several thin-film semiconductors and molecular crystals as noted by Fratini and Troisi [2,31]. In this section, the P_{TRF} is proposed based on the statistical nature of transport with a path length having a distribution on either side of the mean [32]. Roughly, for carriers with path lengths between scattering events greater than or equal to the lattice constant, the use of the BTE with scattering times and associated mobilities due to various scattering mechanisms is justified, while for carriers with path lengths less than the lattice constant, transport can be better described as hopping. We first describe the BTE and how it is used to calculate band mobility due to various scattering mechanisms, then include the effects of multiple trap and release (MTR) in semiconductors with disorder, and finally show how the P_{TRF} is applied.

A. Boltzmann transport equation solved by relaxation time approximation

In semiconductors, the BTE can be applied to calculate the distribution function of the carriers, which is used to get various transport quantities. The BTE is expressed as [33]

$$\frac{\partial f}{\partial t} + \frac{\hbar \vec{k}}{m^*} \cdot \vec{\nabla}_{\vec{r}} f + \frac{-e\vec{F}}{\hbar} \cdot \vec{\nabla}_{\vec{k}} f = \left(\frac{\partial f}{\partial t} \right)_{coll}, \quad (1)$$

where $\hbar$ is the reduced Planck's constant, m^* is the effective mass of the carrier, e is the elementary charge, f is the distribution function, $\vec{r}$ is the position vector, $\vec{k}$ is the wave vector, $\vec{F}$ is the electric field, and $(\partial f / \partial t)_{coll}$ is the collision (scattering) integral.

In the RTA, the total distribution function can be split into a symmetric term f_S and an asymmetric term f_A

$$f = f_S + f_A. \quad (2)$$

We assume the system is under low field, $f_A \ll f_S$ and $f_S \approx f_0$, where f_0 is the Fermi function under equilibrium and the distribution f can be estimated as
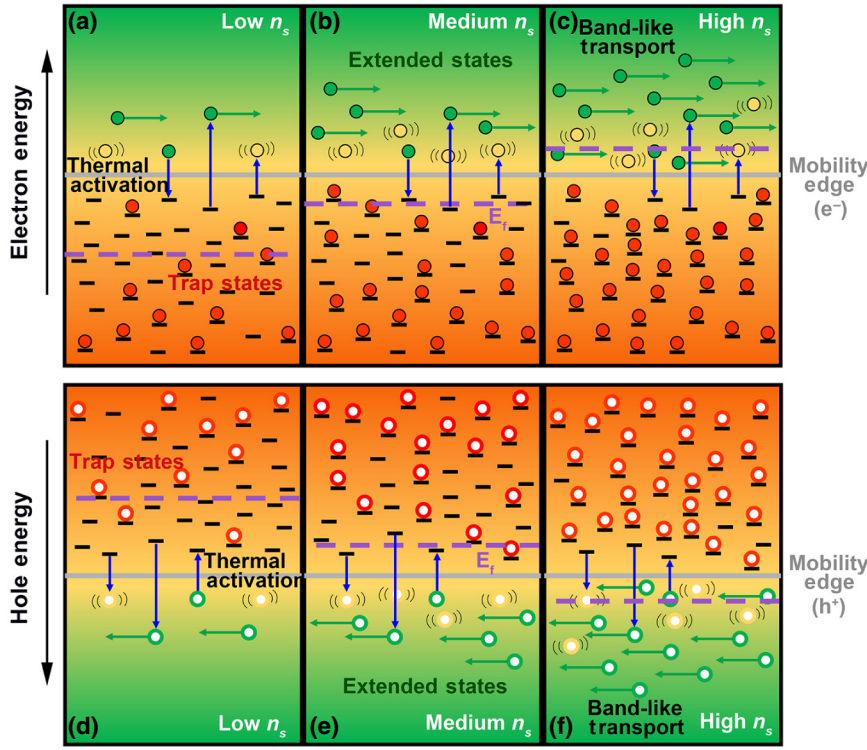
$$f \approx f_0 + f_A. \quad (3)$$

FIG. 2. Schematic illustration of three different types of carriers in the polymer semiconductor at different carrier densities n_s. (a), (b), and (c) show low, medium, and high electron densities, respectively, for n type polymers. (d), (e), and (f) show low, medium, and high hole concentrations, respectively, for p type polymers. The Fermi level is indicated as a purple dashed line. The mobility edge is represented by a gray solid line. Carriers shown in red are in the trap states; those in yellow are thermally excited carriers within the band, but with an inadequate mean free path to contribute to band transport so that they only contribute to screening, and those in green are thermally excited mobile carriers in the band with larger mean free paths that allow band transport.

Thus, the BTE can be approximated as

$$\frac{\partial f}{\partial t} + \frac{\hbar \vec{k}}{m^*} \cdot \vec{\nabla}_{\vec{r}} f + \frac{e\vec{F}}{\hbar} \cdot \vec{\nabla}_{\vec{k}} f = \frac{-f_A}{\tau(k)} \approx \frac{-(f - f_0)}{\tau(k)}, \quad (4)$$

where f_0 is the Fermi function under equilibrium and $\tau(k)$ is momentum relaxation time as a function of k.

If we consider steady-state transport under a uniform electric field, then

$$\frac{\partial f}{\partial t} = 0, \text{ and } \vec{\nabla}_{\vec{r}} f = 0. \quad (5)$$

And since the electric field is low ($f_A \ll f_S$ and $f_0 \approx f_S$), the BTE can be reduced to

$$\frac{-e}{\hbar} \vec{F} \cdot \vec{\nabla}_{\vec{k}} f_0 = \frac{-f_A}{\tau(k)}. \quad (6)$$

Thus, by assuming the electric field is along the z direction

$$f_A = \tau(k) \frac{e}{\hbar} F \frac{\partial f_0}{\partial k_z}. \quad (7)$$

From Eq. (7), the solution of BTE can be obtained as

$$f = f_0 + \tau(k) \frac{e}{\hbar} F \frac{\partial f_0}{\partial k_z}. \quad (8)$$

The second term resembles the linear term in the Taylor series expansion of the distribution function f.

From the distribution function, the average drift velocity $\langle v_d \rangle$ is calculated as

$$\langle v_d \rangle = \frac{-\sum_k \frac{\hbar^2 k^2}{2m^*} \tau(k) \frac{eF}{m^*} f_0}{\langle E \rangle} = \frac{-eF}{m^*} \frac{\langle E\tau(E) \rangle}{\langle E \rangle}, \quad (9)$$

where E is the energy of the carriers. Thus, the band mobility is estimated as

$$\mu_{\text{band}} = \frac{e}{m^*} \frac{\langle E\tau(E) \rangle}{\langle E \rangle}. \quad (10)$$

The above equation serves as the basis to calculate the mobilities due to the various scattering mechanisms.

B. Momentum relaxation time: scattering mechanisms

Band transport in the extended MTR model [1] has several dominant scattering mechanisms. The main scattering mechanisms for this semiconductor system are trapped carrier (TC) scattering, polar optical phonon (LO) scattering, optical deformation potential (ODP) scattering, and acoustic phonon (AC) scattering.

Trapped carriers are highly localized and can be regarded as charged Coulomb scattering centers. These are very efficient scattering centers due to the high degree of special overlap with mobile carriers. The trapped carrier

scattering rate is evaluated as [1,34]

$$\frac{1}{\tau_{\text{TC}}} = n_{\text{trap}} \frac{2\pi}{\hbar} \frac{1}{(2\pi)^2} \iint d^2 k' \frac{|\langle \psi_{\vec{k}} | V_{\text{TC}} | \psi_{\vec{k'}} \rangle|^2}{\varepsilon_{2\text{D}}^2}$$
$$\times \left(1 - \frac{\vec{k} \cdot \vec{k'}}{|\vec{k}|^2} \right) \delta(E_k - E_{k'}), \tag{11}$$

where $\psi_{\vec{k}}$ is the carrier wave function, n_{trap} is the density of trapped charge carriers, V_{TC} is the Coulomb potential of trapped charged carriers, $\varepsilon_{2\text{D}}$ is the screening dielectric function, $\delta(\dots)$ is the Dirac delta function, and E_k $E_{k'}$ are the carrier energies for states k and k', respectively.

The unscreened trapped charge Coulomb potential V_{TC} is described as

$$V_{\text{TC}} = -\frac{e}{4\pi\epsilon_0\epsilon_s\sqrt{r^2 + z^2}}, \tag{12}$$

where ϵ_0 is the vacuum permittivity, ϵ_s is the dielectric constant of the semiconductor, r is the in-plane distance, and z is the out of-plane distance.

At a finite temperature T, the static screening dielectric function $\varepsilon_{2\text{D}}$ for a two-dimensional (2D) carrier gas is described by the Lindard function [35]

$$\varepsilon_{2\text{D}}(q, T, E_k) = 1 + \frac{e^2}{2\epsilon_0\epsilon_s q} \Phi \Pi(q, T, E_k), \tag{13}$$

where q is the 2D scattering wave vector, Φ is the form factor including the effect of dielectric mismatch, which is defined by the equations

$$\Phi = \int\int dz dz' \chi^2(z) \chi^2(z') [-2q\epsilon_0\epsilon_e G_q(z, z')], \tag{14}$$

where $\chi(z)$ is the confined carrier wave function at the interface of the semiconductor and gate dielectric, ϵ_e is the average dielectric constant expressed as $\epsilon_e = (\epsilon_s + \epsilon_{\text{ox}})/2$, ϵ_{ox} is the dielectric constant of gate oxide, and $G_q(z, z')$ is the Green's function for the Poisson equation

$$G_q(z, z') = -\frac{1}{2q\epsilon_0\epsilon_s} \left[\exp(-q|z - z'|) \right.$$
$$\left. + \frac{\epsilon_s - \epsilon_{\text{ox}}}{\epsilon_s + \epsilon_{\text{ox}}} \exp(-q|z + z'|) \right]. \tag{15}$$

Π is the polarizability function of the static state at finite temperature T based on the work of Maldague [35]

$$\Pi(q, T, E_k) = \int \frac{\Pi(q, 0, E'_k)}{4k_B T \cosh^2\left[\frac{E_k - E'_k}{2k_B T}\right]} dE'_k, \tag{16}$$

where k_B is the Boltzmann constant and the $\Pi(q, 0, E)$ is the polarizability function of the static state at zero

temperature given by following [35]

$$\Pi(q, 0, E_k) = \frac{gm^*}{2\pi\hbar^2} \left\{ 1 - \Theta[q - 2k]\sqrt{1 - \left(\frac{2k}{q}\right)^2} \right\}, \tag{17}$$

where g is the degeneracy factors and $\Theta[\dots]$ is the Heaviside unit-step function.

Trapped carrier scattering is dominant at low temperatures because of two reasons: (i) scattering due to phonons is less efficient at low temperature and (ii) more carriers are trapped and function as scattering centers due to less thermal excitation.

Polar optical phonon scattering is prevalent in polar semiconductors. Polymers and amorphous metal oxides also have polar optical phonon mode [36,37], which can affect the carrier transport. The carrier-polar phonon scattering rate is evaluated as

$$\frac{1}{\tau_{\text{LO}}^{\pm}} = \frac{e^2 \omega_{\text{LO}} m^*}{8\pi\hbar^2} \frac{1}{\epsilon_0} \left(\frac{1}{\epsilon_\infty} - \frac{1}{\epsilon_s} \right) \left(N_q + \frac{1}{2} \pm \frac{1}{2} \right)$$
$$\times \int_{-\pi}^{\pi} \frac{1}{q} \frac{\Phi}{\varepsilon_{2\text{D}}^2} \left(1 - \frac{\vec{k} \cdot \vec{k'}}{|\vec{k}|^2} \right) d\theta, \tag{18}$$

where ω_{LO} is the longitudinal optical phonon frequency, ϵ_∞ is the semiconductor dielectric constant at high frequency, $N_q = 1/[\exp(\hbar\omega/k_B T) - 1]$ is the Bose-Einstein distribution, q is the scattering wave vector, and θ is the scattering angle.

Another dominant scattering at high temperature, for example, near or above room temperature, is ODP scattering. Optical phonons, which have a frequency on the order of 10 meV or more, lead to inelastic deformation potential scattering to the carriers. In some polymer materials, the optical phonon frequency can be very low [38,39], leading to a large phonon-carrier scattering rate in the high-temperature range. The scattering rate due to the ODP is given by

$$\frac{1}{\tau_{\text{OP}}^{\pm}} = \frac{D_{\text{OP}}^2 m^* \left(N_q + \frac{1}{2} \pm \frac{1}{2} \right)}{4\pi\hbar^2 \rho_s \omega_{\text{OP}}} \int_{-\pi}^{\pi} \frac{1}{\varepsilon_{2\text{D}}^2} \left(1 - \frac{\vec{k} \cdot \vec{k'}}{|\vec{k}|^2} \right) d\theta, \tag{19}$$

where D_{OP} is the optical deformation potential, ρ_s is the areal mass density, and ω_{OP} is the optical phonon frequency.

Acoustic phonon scattering is also of relevance to the semiconductors in this study. In analogy with ODP scattering, acoustic phonons scattering of carriers is characterized by the acoustic deformation potential. Since the energy of acoustic phonons is very small compared to the energy of carriers, the scattering process between acoustic phonons

and charge carriers can be regarded as elastic. Thus, the scattering rate can be calculated as [34]

$$\frac{1}{\tau_{AC}} = \frac{\Xi_{AC}^2 k_B T m^*}{2\pi \hbar^3 \rho_s v_s^2} \int_{-\pi}^{\pi} \left(1 - \frac{\vec{k} \cdot \vec{k'}}{|\vec{k}|^2}\right) d\theta, \qquad (20)$$

where Ξ_{AC} is the acoustic deformation potential and v_s is the sound velocity in the material.

According to our calculations, acoustic phonon scattering is less significant than the ODP scattering. We note that the detailed studies and measurements of phonon energies and deformation potentials of thin-film semiconductors such as amorphous metal oxides and conjugated polymers are still in progress; hence, there is some uncertainty in calculating the exact scattering rates.

The mobilities limited by each scattering mechanism can be calculated as described above. The total band mobility due to multiple scattering mechanisms can be estimated by Matthiessen's rule

$$\frac{1}{\mu_{band}} = \frac{1}{\mu_{TC}} + \frac{1}{\mu_{LO}} + \frac{1}{\mu_{OP}} + \frac{1}{\mu_{AC}}, \qquad (21)$$

where μ_{TC} is the TC scattering limited mobility, μ_{LO} is the LO phonon scattering limited mobility, μ_{OP} is the optical phonon deformation potential scattering mobility limited, and μ_{AC} is acoustic phonon scattering limited mobility.

C. Multiple trap and release

The MTR model has been widely applied to analyze transport in thin-film semiconductor systems since the defects play an important role in carrier transport [18,40,41]. The MTR effective mobility is the band mobility multiplied by the fraction of carriers in the band that are above the mobility edge. We note that the band edge is the highest energy possible for the mobility edge and in our work the band edge and mobility edge are assumed to be at the same energy.

$$\mu_{MTR} = \mu_{band} \frac{n_{band}}{n_{trap} + n_{band}}, \qquad (22)$$

where n_{band} is the carrier concentration in the band. The detailed calculation of n_{band} and n_{trap} is described in Appendix A: Density of states.

D. Transport reduction factor

We define the P_{TRF} as the probability $p(a)$ that a carrier will traverse a distance of a or greater, $p(a)$ [32], based on the mean free path of the carrier L_{MFP} with the band

transport model,

$$P_{TRF}(L_{MFP}) \equiv p(a) = e^{-(a/L_{MFP})}. \qquad (23)$$

L_{MFP}, in turn, can be estimated as [42]

$$L_{MFP} = v_c \cdot \tau = \frac{\mu_{band}\sqrt{2m^* E_k}}{e}, \qquad (24)$$

where v_c is the average (thermal) carrier velocity magnitude in one dimension as appropriate for transport in molecular chains as considered here, τ is the average free flight time (relaxation time) of the carriers, μ_{band} is the carrier mobility in the band, and E_k is the carrier energy above the band edge and is given by $k_B T$. In our calculations, carriers with path length $\leq a$ are modeled as localized and carriers with path length $> a$ are modeled as delocalized.

The P_{TRF} bridges two limits of the transport. When L_{MFP} is very large compared to a, the P_{TRF} is close to unity, which means that carriers in the band are essentially delocalized and the transport can be described properly by Boltzmann transport theory. When the calculated L_{MFP} is very small compared to a, the P_{TRF} value will also be very small, which means that all carriers are strongly localized and can move only by hopping, that is, that there is essentially no mobility edge. This latter limit is observed in disordered organic semiconductor material systems such as amorphous polymers and molecular doped polymers [28,43]. When L_{MFP} is on the order of the intermolecular distance, the P_{TRF} represents the degree to which carriers participate in band transport versus the degree to which they move by hopping. That is, effectively, the fraction of particles that participate in band transport as describable by the BTE versus the fraction that are effectively localized but still may move by hopping and contribute to screening. In Fig. 2, we represent carriers with inadequate paths lengths by yellow circles. Thus, the P_{TRF} is a useful phenomenological construct that can help integrate band and hopping transport theories. However, while the P_{TRF} is phenomenological, it is rooted in the statistical basis of charge transport. Our focus in this paper is on the band transport, and while noting that it exists, we do not consider hopping transport explicitly. In some organic semiconductors, it has been stated that band transport and hopping both are important [44]. In future work, we will clarify how both band and hopping transport must be treated together.

For this work, only low electric fields are considered and the carrier velocity magnitude is determined solely by the thermal energy. The carrier relaxation time is derived from the scattering rate, which is also influenced by the temperature and carrier concentration. Therefore, the P_{TRF} is highly dependent on two variables: temperature and carrier concentration (the latter dependent on gate voltage). For polymers, the threshold distance for carriers to participate

in band transport is typically the ring-to-ring intermolecular distance (approximately 0.3 nm). This distance can be considered as corresponding to the lattice constant in inorganic semiconductors.

However, when eliminating these latter low-mean free path carriers from consideration for band transport by the P_{TRF}, what remains are carriers with mean free paths, and thus, mobility greater than would be predicted for all particles as a whole. Since paths of nominal free path lengths less than a are eliminated from the band transport model via the P_{TRF}, and the distribution of path lengths for the remaining carriers continues to follow the Poisson distribution, the mean free path for the remaining carriers $L_{MFP \text{-} eff}$ relative to the nominal mean free path L_{MFP} increases simply as

$$\frac{L_{MFP \text{-} eff}}{L_{MFP}} = \frac{a + L_{MFP}}{L_{MFP}} = 1 + \frac{a}{L_{MFP}} = 1 - \ln(P_{TRF}).$$
$$(25)$$

With the time between scattering events, and thus, mobility for these long mean free path carriers scaling with this effective mean free path $L_{MFP \text{-} eff}$, but also with the fraction of carriers available for BTE-based transport as characterized by the subunity P_{TRF}, and with the subunity fraction of carriers above the mobility edge, the experimentally measurable mobility in terms of all carriers becomes

$$\mu_{TRF} = \mu_{band} \frac{n_{band}}{n_{trap} + n_{band}} P_{TRF}[1 - \ln(P_{TRF})]$$
$$= \mu_{MTR} P_{TRF}[1 - \ln(P_{TRF})]. \qquad (26)$$

The reduction of mobility due to P_{TRF} is estimated as above. For example, when $L_{MFP} = a$, $P_{TRF} = e^{-1} \cong 0.37$ and when $P_{TRF}[1 - \ln(P_{TRF})] = e^{-1}[1 + 1] \cong 0.74$.

The P_{TRF} describes the degree of effective localization of free carriers in the band due to strong scattering. Introduction of this factor is one of the main points of this article, which allows us to create a proper theoretical framework with which to analyze transport in semiconductors with mobilities that fall between regimes for which hopping transport theories and band transport theories apply. Several such semiconductors have been reported in recent years including those that exhibit a normal Hall Effect, which is a strong indicator of delocalized transport [44,45]. The P_{TRF} defined here is shown as a function of mean free path length for exemplary intermolecular distance and/or lattice constant values in Fig. 3.

E. Range of validity of our approach

Our approach will work when polaron theory does not apply. Kenkre *et al.* have proposed that polaron theory will not apply for semiconductors when $g^2 \hbar \omega / BW$ is < 1, where BW is the electronic band width, g is the dimensionless electron-phonon coupling constant, and ω is the
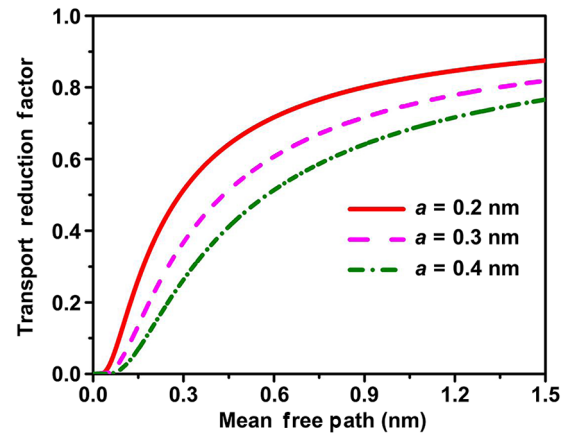

FIG. 3. Illustration of P_{TRF} as a function of mean free path for different examples of intermolecular distance a. The function is related to the probability of a carrier that can traverse the intermolecular distance on average. This probability follows the Poisson distribution. For a certain mean free path value, the P_{TRF} increases when the intermolecular distance is small. And for a fixed intermolecular distance, the value of the P_{TRF} decreases as the mean free path decreases.

frequency of the dominant phonon mode [30]. This criterion essentially means that the electronic band width should be much larger than the phonon energies of the system for polaron theory to not apply. The calculated effective mass along the chain in donor-acceptor polymers, which have relatively strong π bonding, is less than m_0, the free electron mass [46,47]. The effective mass of amorphous oxides such as zinc tin oxide (ZTO) and indium gallium zinc oxide (IGZO) are also less than m_0 [48,49]. Such semiconductors will have a relatively large electronic band width as a result. Our approach will be valid for such systems.

III. RESULTS AND DISCUSSION

A. Device structure

To illustrate our analysis, we compare our calculations with experimental data from TFTs based on the diketopyrrolopyrrole (DPP) [50] polymer, whose structure is shown in Fig. 4(a) Additional details of the device structure shown in Fig. 4(b) and materials employed are provided in Table I. Similar polymers have demonstrated mobilities in the range 1–20 cm²/(Vs) in numerous reports published in the past decade [51–53]. Charge transport in such semiconductors has usually been described by the MTR model as described above [1,40,41].

B. Results of mobility calculations

We calculate carrier mobility in the RTA solution of the BTE considering all main scattering mechanisms, as described in Sec. II. The main scattering mechanism in
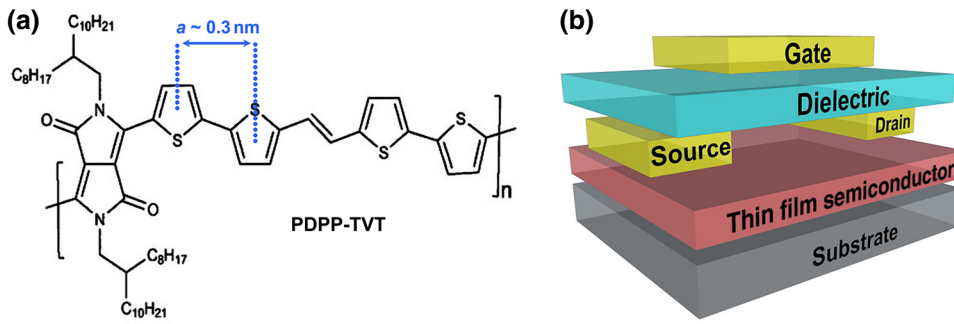
(a)

(b)

FIG. 4. Molecular structure of PDPP-TVT and thin-film device structure. (a) Shows the PDPP-TVT molecular structure where the ring to ring distance a (intermolecular distance) is around 0.3 nm. (b) The device structure of thin-film transistor [50]. A top gate structure is implemented with polymeric insulator D139 as the gate dielectric. The gate capacitance is 4 nF/cm^2. The channel length and width are 50 and 1000 μm, respectively.

these transistors at most temperatures is TC scattering, which again is the scattering of mobile carriers by those that are trapped [1]. At close to room temperature, phonon scattering also becomes significant. The carriers above the mobility edge also screen each other from scattering centers (as shown in green and yellow in Fig. 2). We assume a carrier (hole) effective mass of 0.15 m_0, consistent with recent calculations and experimental data for similar donor-acceptor polymers along the chain [46,47]. From this assumption, the density of states above the band edge is calculated. The density of trap states (DOS) is calculated as a function of energy, assuming that at the band edge there is continuity in the DOS and that the trap DOS decreases exponentially with energy [54]. Details of DOS calculations are described in Appendix A.

The fraction of carriers above the mobility edge, or the MTR factor, is shown in Fig. 5(a) as a function of reciprocal temperature and gate voltage. The rest of the field-induced carriers are in trap states. The P_{TRF} described above characterizes an effective division of carriers above the nominal mobility edge into those that contribute to the current and those that are effectively localized and only provide screening. The division of carriers based on an application of the P_{TRF} and MTR factor is shown in Fig. 5(b). These distributions are functions of temperature and the total induced carrier density. It can be seen that high carrier densities and higher temperatures favor band transport, as is expected.

We now address two of the features that have been closely associated with charge transport in polymer and organic semiconductors: polarization effects and the effects of morphology. As mentioned in Section II, our work is not applicable when molecular polaron effects dominate transport [30]. Dielectric polarization effects, on the other hand, can be significant [55,56]. These arise from polar media such as high K dielectrics or polar molecules in contact with the semiconductor. In such situations, the trap DOS is altered (increased) by the distortion created by polarization. The trap DOS together with the appropriate deformation potential value adequately accounts for polarization effects in systems with relatively low dielectric constant insulators such as SiO$_2$ ($\epsilon_r \sim 3.9$). In other words, polarization effects are included in the deformation potential term and in the DOS. When higher K dielectrics are used, polarization effects can become more severe in polymer semiconductors [56], possibly resulting in effective mass changes. In this work, we do not consider the effects of very large polarizations and possible changes to effective mass. We will address these in future work.

Morphological imperfections manifest as trap states and we make a simplifying assumption that our derived trap density of states accounts for most key features of the morphology, albeit at a higher level. If trapping at domain and/or grain boundaries is significant, as in some small molecule organic TFTs, then the current and hence effective mobility are reduced by the thermal activation across

TABLE I. Parameters used to theoretically calculate the mobility for PDPP-TVT TFT

| Calculation Parameters			
Effective mass	0.15 m_0	Longitudinal optical phonon energy	50 meV
Tail trap density N_t	2.7×10^{16}/cm^2	Effective optical deformation potential	1.9×10^{11} eV/m
Characteristic temperature T_{ta}	500 K	Effective acoustic deformation potential	5 eV
Subthreshold trap density	3.7×10^{15}/cm^2	Sound velocity	2.5×10^3 m/s
PDPP-TVT dielectric constant	4	Mass density	1 g/cm^3
Gate oxide dielectric constant	2.5	Intermolecular distance	0.3 nm
Optical phonon energy	6 meV		

where m_0 is the electron mass.
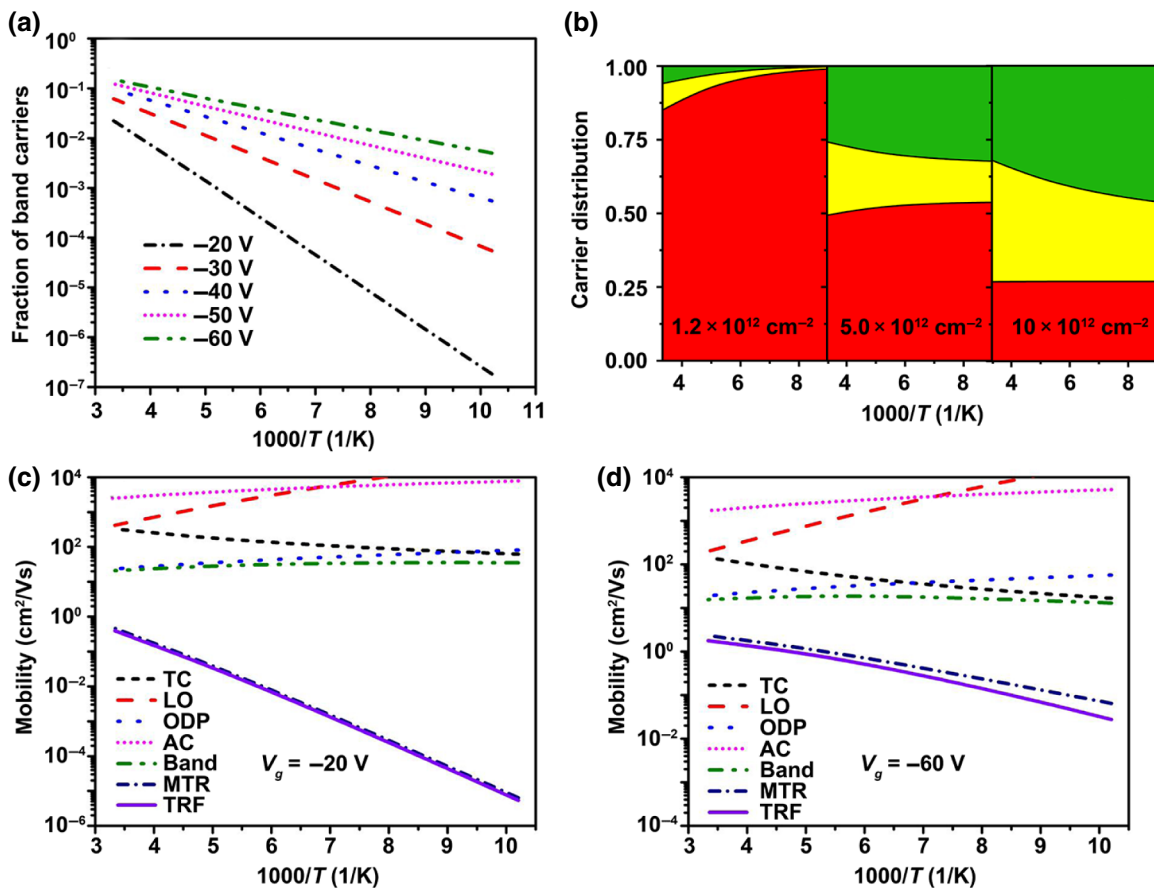
FIG. 5. Carrier distribution and composition of mobilities. (a) Fractions of carriers thermally excited into the band as a function of reciprocal temperature ($1000/T$) for different gate voltages (carrier concentrations). This includes both the carriers with inadequate mean free path and the mobile carriers. The fraction increases with increasing temperature and increasing carrier concentration. (b) Carrier distributions versus $1/T$ for three different carrier concentrations ($n_s = 1.2 \times 10^{12}$ cm^{-2}, 5.0×10^{12} cm^{-2}, and 10×10^{12} cm^{-2}). Red: trapped carriers; Yellow: thermally excited carriers in the band, but with inadequate mean free path; Green: thermally excited mobile carriers in the band, which participate in the band transport process. The density of green mobile carriers increases with carrier concentration. (c) and (d) Mobility calculations for different scattering mechanisms for $V_g = -20$ V and $V_g = -60$ V. (TC-trapped carrier scattering; LO-longitudinal optical phonon scattering; ODP-optical deformation potential scattering; AC-acoustic deformation potential scattering; Band-total band mobility; MTR-apparent mobility due to multiple trap and release; TRF-transport reduction factor corrected mobility.) At high temperature, the band mobility is mainly limited by ODP scattering, and at low temperature, the band mobility is limited by the trapped carrier scattering.

potential barriers that arise from charge trapping [57,58]. In high mobility DPP polymers, the measured "apparent" activation energies are quite small and include contributions from thermal activation from trap to extended states (MTR), the temperature dependence arising from trapped carrier scattering, improved screening due to more carriers excited above the mobility edge, and activation across barriers at grain and/or domain boundaries. We neglect the last factor in this work as it is believed to be fairly small in these high mobility polymers, especially at large carrier densities.

The mobilities due to the important scattering mechanisms are calculated and plotted in Figs. 5(c) and 5(d). The parameter values used are provided in Table I. TC scattering is the most dominant mechanism at temperatures below room temperature. At the carrier densities employed in this study, the band mobility due to TC scattering increases slightly with increasing temperature due to improved screening and a reduction in the trapped carrier density [Fig. 5(a)]. At higher temperatures, ODP scattering is significant in this system. LO phonon scattering and AC scattering have also been considered in our calculations, and are shown in Figs. 5(c) and 5(d). In Figs. 5(c) and 5(d) are also plotted the corrected mobilities due to trap and release and due to the P_{TRF}. We reiterate that the calculated mobility values incorporate the P_{TRF}, the effects of thermal activation from traps (MTR factor), and the effects of various scattering mechanisms. This is the central result
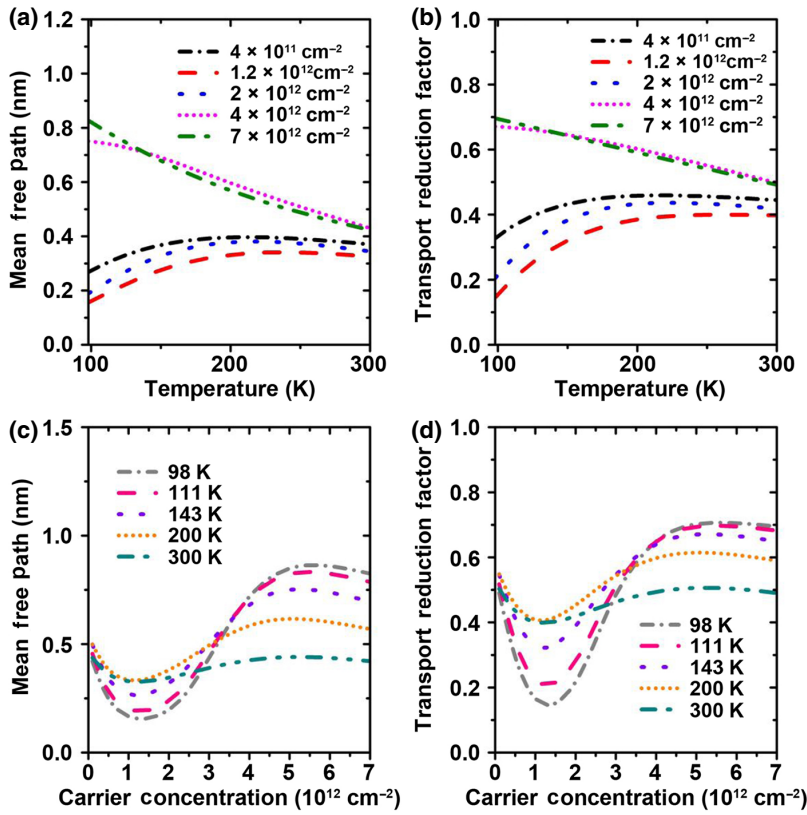
FIG. 6. Mean free path and transport reduction factor for different temperatures and different carrier concentrations. Mean free path is calculated based on the band mobility and the carrier thermal velocity. The mean free path is dependent on the temperature and carrier concentration as shown in (a) and (c). Transport reduction factor is then calculated based on the mean free path. The intermolecular distance is set to be 0.3 nm in the calculation. Temperature and carrier concentration dependent transport reduction factor is shown in (b) and (d).

of our paper and it should apply in all situations in which band transport is prevalent, but the mean free path is not very large. Our calculation procedure will be applicable to many polymer semiconductors and amorphous metal oxide semiconductors.

C. Comparison with experimental data

In Fig. 6, the calculated mean free paths given by Eq. (1) and P_{TRF}s are shown as a function of temperature and carrier density (gate voltage). The shapes of these curves are a consequence of the interdependence of mobility and
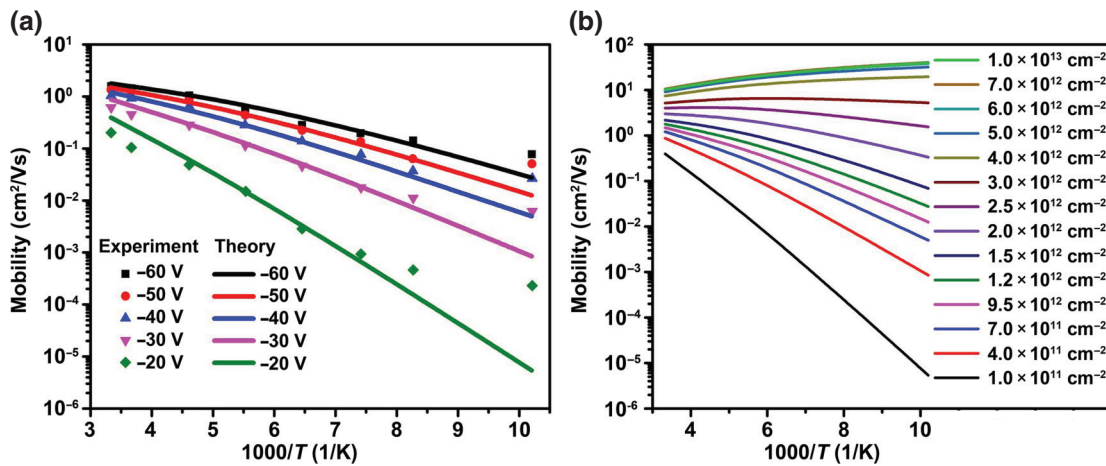

FIG. 7. Fitting to the experimental data and the extended calculation of mobility for higher carrier concentrations. (a) Experimental mobility data fitted with our model with various scattering mechanisms, trap excitation probabilities, and transport reduction factor correction. The effects of morphological imperfections in the polymer film are included in the trap DOS. The fit between theory and experiment is in good agreement [50] across all gate voltages, except for a discrepancy at low temperature. (b) Calculated mobility at increased carrier concentrations. The mobility increases with increasing carrier density, but reaches a plateau at high carrier density ($\sim 7.0 \times 10^{12}$ cm^{-2}). This is due to the ODP scattering enhanced at high carrier density [34]. These mobilities can be further enhanced by selecting more rigid polymers that are less sensitive to polarization effects.

carrier density in the band on temperature and also on the gate voltage. We compare experimental results previously published by our group with this calculation in Fig. 7(a) [50]. The agreement is good with some discrepancy at low temperatures. This could arise from local heating of the samples during measurement, an effect that is relatively stronger at lower temperatures. We have also calculated the effect of increasing the carrier density on mobility in the samples considered for Fig. 7(b). The mobility increases substantially, especially at low temperatures. This result validates the use of bilayer gate dielectrics to increase mobility by increasing the carrier density without enhancing polarization effects [59]. Further increases in mobility at room temperature can come from reduced ODP and/or phonon scattering by improvements in molecular design. Reducing the TC density is also extremely important to get larger mobilities in thin-film transistors, not just in terms of MTR, but because associated reduction in scattering centers and more screening also produce a larger P_{TRF}.

While our illustrative example is a polymer TFT, the approach we have described is more widely applicable. In principle, it should apply in all situations for which the mean free path is comparable to the intermolecular length or lattice constant and where the polaron effects can be neglected. The scattering mechanisms will, of course, be material specific. Our framework also allows us to combine hopping and band transport in a quantitative if not a phenomenological manner to generate a comprehensive transport picture. Furthermore, we have explicitly shown how to include the effects of MTR, which is ubiquitous in disordered systems with at least some degree of band transport. In the Supplemental Material [60], we have successfully applied our calculation procedure to data from a polymer with mobility greater than 10 cm^2/(Vs) at room temperature [24].

IV. CONCLUSION

In summary, we present an alternative theoretical framework with which to analyze charge transport in a variety of TFTs in which the room temperature mobility is in the range 1–20 cm^2/(Vs). This range is typical for many TFTs that have been reported in recent years. We have pointed out the necessity of including a P_{TRF} to account for carriers strongly localized by scattering even if above the nominal mobility edge. We use this factor as the basis of reinterpreting the mobility edge in TFTs. We illustrate our analysis by a comparison with experimental data from polymer TFTs, which are believed to possess relatively low effective mass along the polymer chain. Scattering mechanisms specific to such polymer TFTs are evaluated. For such materials, TC scattering is dominant below room temperature while close to room temperature and above it, phonon scattering including deformation potential scattering is important.

APPENDIX A: DENSITY OF STATES

Thin-film transistors usually work in the accumulation region. In this region, the carrier energy levels are quantized at the semiconductor-insulator interface due to the formation of triangular potential wells by gate dielectric and valence band (conduction band for electron) potential [61]. Thus, the carriers induced at interface should be treated as a 2D carrier gas and the confined wave function at the interface can be described by the Airy function. Taking the hole transport as an example, the transport of holes happens at valence band maxima (conduction band minima for electrons), thus a parabolic band energy dispersion relation is applied. Therefore, the band density of states (DOS) for holes is given by

$$N_{\text{band}}(E) = \frac{gm^*}{2\pi\hbar^2} \quad (E_k < E_v), \tag{A1}$$

where g is the degeneracy factor, E_k is the hole energy, and E_v is the valence band edge energy.

Disordered thin-film semiconductors such as polymers and organic molecules have significant DOSs [62]. The trap states' DOS is assumed to have a continuous exponentially decaying tail below the band edge [63,64]

$$N_{\text{trap}}(E) = \frac{N_t}{k_B T_{ta}} e^{(E_v - E_k)/k_B T_{ta}} \quad (E_k > E_v), \tag{A2}$$

where N_t is the total trap density and T_{ta} is the characteristic temperature of the trap DOS. The DOS configuration used in the calculation for diketopyrrolopyrrole–thienylene–vinylene–thienylene copolymer (PDPP-TVT) thin-film transistor is shown in Fig. 8(a).

Based on the DOS and the Fermi level E_f at certain temperature T, the TC concentration and the density of carriers thermally excited into the band can be calculated as

$$n_{\text{trap}} = \int_{E_v}^{\infty} \frac{N_t}{k_B T_{ta}} e^{(E_v - E_k)/k_B T_{ta}} f_{\text{FD}}(E_k - E_f) dE_k, \tag{A3}$$

$$n_{\text{band}} = \int_{-\infty}^{E_v} \frac{gm^*}{2\pi\hbar^2} f_{\text{FD}}(E_k - E_f) dE_k, \tag{A4}$$

where $f_{\text{FD}} = 1/\{1 + \exp[(E_k - E_f)/k_B T]\}$ is the Fermi-Dirac distribution. n_{trap} is the density of charged immobile
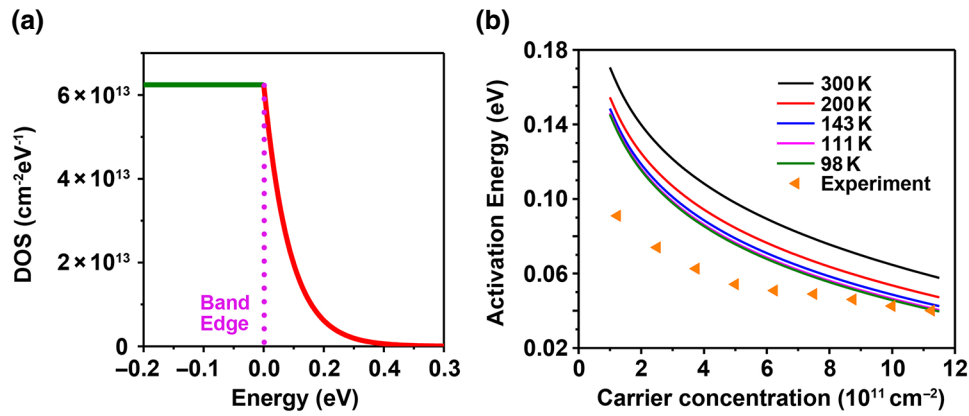
(a)

(b)

FIG. 8. DOS and activation energy. (a) Configuration of DOS used in calculation for PDPP-TVT TFT. Green line indicates the 2D DOS in the valance band; Red line illustrates the exponentially decayed tail trap states in the band gap. At the band edge (mobility edge), indicated by purple dotted line, the DOS is assumed to be continuous by mathematical simplicity. (b) Activation energy from experiment and theory. The activation energy extracted from experimental data is smaller than the theoretically calculated ones at most carrier concentrations. Higher temperature results in higher activation energy from the calculations.

carriers in the trap states. It contributes to the Coulomb scattering as discussed earlier in Sec. II. n_{band} is the concentration of untrapped carriers. However, statistically, in thin-film semiconductors that have a mobility of 1–20 cm^2/(Vs), not all of those carriers can have band transport. Due to serious scattering, some of the carriers have very small free paths and are effectively localized in a lattice range. Band transport is highly unlikely for those carriers. On the other hand, there is still a fraction of carriers with large enough free paths that participate in the band transport. The transport reduction factor is used to portray this picture by estimating the fraction of carriers with large free paths.

APPENDIX B: MTR MODEL USED IN EXPERIMENT AND ACTIVATION ENERGY

The energy that carriers require to get thermally excited into the band or above the mobility edge from the trap state is defined as activation energy in the thin-film semiconductor. The activation energy is usually extracted from the experimentally measured temperature-dependent mobility based on the assumption of a simple MTR model [62,65]

$$\mu = \mu_0 e^{-(E_a/k_B T)}, \tag{B1}$$

where μ is measured "apparent" mobility, μ_0 is the band mobility, and E_a is the activation energy.

This simple model has two limitations in describing the whole picture of the MTR transport mechanism. First, the statistical function used in this model is based on a Boltzmann distribution. When the thin-film semiconductor is not degenerate or the Fermi level is quite far away from the band edge, Boltzmann statistics are a good approximation to Fermi-Dirac statistics. However, when the thin-film semiconductor is degenerate or the Fermi level is very

close to the band edge, which is the usual case in the accumulation region when the thin-film transistor is operating, Boltzmann statistics will result in a large deviation in the extracted activation energy. Second, most analyses treat μ_0 as a constant value when extracting the activation energy from experimental data [5]; however, μ_0 is temperature dependent, especially at high carrier concentration. The band mobility is determined by several scattering mechanisms, which are discussed in Section II and has a nonconstant value over the temperature. Ignoring both these factors will lead to an inaccurate activation energy extraction. In order to get a more accurate extraction of activation energy in the MTR model, band mobility calculations and Fermi-Dirac statistics must be implemented. Figure 8(b) shows the comparison between the experimentally extracted activation energy based on a simple MTR model and the calculated activation energy from theory. The activation energies should not be the same for different temperatures due to the temperature dependence of the Fermi-Dirac distribution.

[1] X. Wang and A. Dodabalapur, Trapped carrier scattering and charge transport in high-mobility amorphous metal oxide thin-film transistors, Ann. Der Phys. **530,** 1800341 (2018).

[2] S. Fratini, D. Mayou, and S. Ciuchi, The transient localization scenario for charge transport in crystalline organic materials, Adv. Funct. Mater. **26,** 2292 (2016).

[3] W. Li, Electrical transport limited by electron-phonon coupling from Boltzmann transport equation: An ab initio study of Si, Al, and MoS$_2$, Phys. Rev. B **92,** 075405 (2015).

[4] N. Cavassilas, F. Aniel, G. Fishman, and R. Adde, Full-band matrix solution of the Boltzmann transport equation and electron impact ionization in GaAs, Solid State Electron. **46,** 559 (2002).

[5] C. G. Lee, B. Cobb, and A. Dodabalapur, Band transport and mobility edge in amorphous solution-processed zinc tin oxide thin-film transistors, Appl. Phys. Lett. **97**, 203505 (2010).

[6] S. N. Mott, The mobility edge since 1967, J. Phys. C: Solid State Phys. **20**, 3075 (1987).

[7] S. N. Mott, in *Phys. Hydrog. Amorph. Silicon II* (Springer, Berlin, Heidelberg, 1984), pp. 169–193.

[8] A. F. Paterson, N. D. Treat, W. Zhang, Z. Fei, G. Wyatt-Moon, H. Faber, G. Vourlias, P. A. Patsalas, O. Solomeshch, N. Tessler, M. Heeney, and T. D. Anthopoulos, Small molecule/polymer blend organic transistors with hole mobility exceeding 13 cm^2 V^{-1} s^{-1}, Adv. Mater. **28**, 7791 (2016).

[9] H. Bronstein, Z. Chen, R. S. Ashraf, W. Zhang, J. Du, J. R. Durrant, P. Shakya Tuladhar, K. Song, S. E. Watkins, Y. Geerts, M. M. Wienk, R. A. J. Janssen, T. Anthopoulos, H. Sirringhaus, M. Heeney, and I. McCulloch, Thieno[3,2- b]thiophene-diketopyrrolopyrrole-containing polymers for high-performance organic field-effect transistors and organic photovoltaic devices, J. Am. Chem. Soc. **133**, 3272 (2011).

[10] P. Barquinha, A. M. Vila, G. Gonçalves, L. Pereira, R. Martins, J. R. Morante, and E. Fortunato, Gallium-indium-zinc-oxide-based thin-film transistors: Influence of the source/drain material, IEEE Trans. Electron Devices **55**, 954 (2008).

[11] E. M. C. Fortunato, P. M. C. Barquinha, A. C. M. B. G. Pimentel, A. M. F. Gonçalves, A. J. S. Marques, L. M. N. Pereira, and R. F. P. Martins, Fully transparent ZnO thin-film transistor produced at room temperature, Adv. Mater. **17**, 590 (2005).

[12] J. H. Cho, J. Lee, Y. Xia, B. Kim, Y. He, M. J. Renn, T. P. Lodge, and C. Daniel Frisbie, Printable ion-gel gate dielectrics for low-voltage polymer thin-film transistors on plastic, Nat. Mater. **7**, 900 (2008).

[13] J. H. Cho, J. Lee, Y. He, B. Kim, T. P. Lodge, and C. D. Frisbie, High-capacitance ion gel gate dielectrics with faster polarization response times for organic thin film transistors, Adv. Mater. **20**, 686 (2008).

[14] S. H. Lee, T. Kim, J. Lee, C. Avis, and J. Jang, Solution-processed gadolinium doped indium-oxide thin-film transistors with oxide passivation, Appl. Phys. Lett. **110**, 122102 (2017).

[15] E. G. Bittle, J. I. Basham, T. N. Jackson, O. D. Jurchescu, and D. J. Gundlach, Mobility overestimation due to gated contacts in organic field-effect transistors, Nat. Commun. **7**, 10908 (2016).

[16] Y. Mei, M. A. Loth, M. Payne, W. Zhang, J. Smith, C. S. Day, S. R. Parkin, M. Heeney, I. McCulloch, T. D. Anthopoulos, J. E. Anthony, and O. D. Jurchescu, High mobility field-effect transistors with versatile processing from a small-molecule organic semiconductor, Adv. Mater. **25**, 4352 (2013).

[17] E. G. Bittle, H. W. Ro, C. R. Snyder, S. Engmann, R. J. Kline, X. Zhang, O. D. Jurchescu, D. M. DeLongchamp, and D. J. Gundlach, Dependence of electrical performance on structural organization in polymer field effect transistors, J. Polym. Sci. Part B: Polym. Phys. **55**, 1063 (2017).

[18] L. Schulz, E.-J. Yun, and A. Dodabalapur, Effects of contact resistance on the evaluation of charge carrier mobilities and transport parameters in amorphous zinc tin oxide thin-film transistors, Appl. Phys. A **115**, 1103 (2014).

[19] H. T. Yi, M. M. Payne, J. E. Anthony, and V. Podzorov, Ultra-flexible solution-processed organic field-effect transistors, Nat. Commun. **3**, 1259 (2012).

[20] Y. Chen, H. T. Yi, and V. Podzorov, High-Resolution ac Measurements of the Hall Effect in Organic Field-Effect Transistors, Phys. Rev. Appl. **5**, 034008 (2016).

[21] Z. Wang, Z. Liu, L. Ning, M. Xiao, Y. Yi, Z. Cai, A. Sadhanala, G. Zhang, W. Chen, H. Sirringhaus, and D. Zhang, Charge mobility enhancement for conjugated DPP-selenophene polymer by simply replacing one bulky branching alkyl chain with linear one at each DPP unit, Chem. Mater. **30**, 3090 (2018).

[22] K. K. Banger, Y. Yamashita, K. Mori, R. L. Peterson, T. Leedham, J. Rickard, and H. Sirringhaus, Low-temperature, high-performance solution-processed metal oxide thin-film transistors formed by a "sol-gel on chip" process, Nat. Mater. **10**, 45 (2011).

[23] Y. Yamashita, J. Tsurumi, F. Hinkel, Y. Okada, J. Soeda, W. Zajączkowski, M. Baumgarten, W. Pisula, H. Matsui, K. Müllen, and J. Takeya, Transition between band and hopping transport in polymer field-effect transistors, Adv. Mater. **26**, 8169 (2014).

[24] Y. Yamashita, F. Hinkel, T. Marszalek, W. Zajaczkowski, W. Pisula, M. Baumgarten, H. Matsui, K. Mu, and J. Takeya, Mobility exceeding 10 cm^2/(V·s) in donor—acceptor polymer transistors with band-like charge transport, Chem. Mater. **28**, 420 (2016).

[25] M. Nikolka, G. Schweicher, J. Armitage, I. Nasrallah, C. Jellett, Z. Guo, M. Hurhangee, A. Sadhanala, I. Mcculloch, and C. B. Nielsen, Performance improvements in conjugated polymer devices by removal of water-induced traps, Adv. Mater. **30**, 1801874 (2018).

[26] J. Il Park, J. W. Chung, J. Y. Kim, J. Lee, J. Y. Jung, B. Koo, B. L. Lee, S. W. Lee, Y. W. Jin, and S. Y. Lee, Dibenzothiopheno[6,5-b:6′,5′-f]thieno[3,2-b]thiophene (DBTTT): High-performance small-molecule organic semiconductor for field-effect transistors, J. Am. Chem. Soc. **137**, 12175 (2015).

[27] M. Mativenga, S. An, and J. Jang, Bulk accumulation a-IGZO TFT for high current and turn-on voltage uniformity, IEEE Electron Device Lett. **34**, 1533 (2013).

[28] H. Bässler, Charge transport in disordered organic photoconductors a Monte Carlo simulation study, Phys. Status Solidi B **175**, 15 (1993).

[29] S. V. Novikov, D. H. Dunlap, V. M. Kenkre, P. E. Parris, and A. V. Vannikov, Essential Role of Correlations in Governing Charge Transport in Disordered Organic Materials, Phys. Rev. Lett. **81**, 4472 (1998).

[30] V. M. Kenkre, J. D. Andersen, D. H. Dunlap, and C. B. Duke, Unified Theory of the Mobilities of Photoinjected Electrons in Naphthalene, Phys. Rev. Lett. **62**, 1165 (1989).

[31] S. Fratini, S. Ciuchi, D. Mayou, G. T. De Laissardière, and A. Troisi, A map of high-mobility molecular semiconductors, Nat. Mater. **16**, 998 (2017).

[32] R. N. Varney, Mean free paths, ion drift velocities, and the Poisson distribution, Am. J. Phys. **39**, 534 (1971).

[33] M. Lundstron, *Fundamentals of Carrier Transport* (Cambridge University Press, Cambridge, 2000).

[34] N. Ma and D. Jena, Charge Scattering and Mobility in Atomically Thin Semiconductors, Phys. Rev. X **4,** 011043 (2014).

[35] K. Hirakawa and H. Sakaki, Mobility of the two-dimensional electron gas at selectively doped n -type $Al_xGa_{1-x}As/GaAs$ heterojunctions with controlled electron concentrations, Phys. Rev. B **33,** 8291 (1986).

[36] C. Cobet, J. Gasiorowski, R. Menon, K. Hingerl, S. Schlager, M. S. White, H. Neugebauer, N. S. Sariciftci, and P. Stadler, Influence of molecular designs on polaronic and vibrational transitions in a conjugated push- pull copolymer, Sci. Rep. **6,** 35096 (2016).

[37] M. Funaki, K. Makise, B. Shinozaki, K. Yano, F. Utsuno, K. Inoue, and H. Nakamura, Electron-phonon scattering in amorphous In_2O_3-ZnO films, J. Appl. Phys. **103,** 113701 (2008).

[38] J. T. L. Navarrete and G. Zerbi, Lattike dynamics and vibrational and polymer spectra of polythiophene. I: oligomers, J. Chem. Phys. **94,** 957 (1991).

[39] R. Hildner, U. Lemmer, U. Scherf, M. Van Heel, and J. Köhler, Revealing the electron-phonon coupling in a conjugated polymer by single-molecule spectroscopy, Adv. Mater. **19,** 1978 (2007).

[40] G. Horowitz, Organic field-effect transistors, Adv. Mater. **10,** 365 (1998).

[41] G. Horowitz, M. E. Hajlaoui, and R. Hajlaoui, Temperature and gate voltage dependence of hole mobility in polycrystalline oligothiophene thin film transistors, J. Appl. Phys. **87,** 4456 (2000).

[42] S. Kasap and C. Peter, *Springer Handbook of Electronic and Photonic Materials* (Springer International Publishing, New York, NY, 2017).

[43] I. I. Fishchuk, V. I. Arkhipov, A. Kadashchuk, P. Heremans, and H. Bässler, Analytic model of hopping mobility at large charge carrier concentrations in disordered organic semiconductors: Polarons versus bare charge carriers, Phys. Rev. B **76,** 045210 (2007).

[44] H. T. Yi, Y. N. Gartstein, and V. Podzorov, Charge carrier coherence and Hall effect in organic semiconductors, Sci. Rep. **6,** 23650 (2016).

[45] J. Socratous, S. Watanabe, K. K. Banger, C. N. Warwick, R. Branquinho, P. Barquinha, R. Martins, E. Fortunato, and H. Sirringhaus, Energy-dependent relaxation time in quaternary amorphous oxide semiconductors probed by gated Hall effect measurements, Phys. Rev. B **95,** 045208 (2017).

[46] B. B. Hsu, C. Cheng, C. Luo, S. N. Patel, C. Zhong, H. Sun, J. Sherman, B. H. Lee, L. Ying, M. Wang, G. Bazan, M. Chabinyc, J. Brédas, and A. Heeger, The density of states and the transport effective mass in a highly oriented semiconducting polymer: Electronic delocalization in 1D, Adv. Mater. **27,** 7759 (2015).

[47] K. Broch, D. Venkateshvaran, V. Lemaur, Y. Olivier, D. Beljonne, M. Zelazny, I. Nasrallah, D. J. Harkin, M. Statz, R. Di Pietro, A. J. Kronemeijer, and H. Sirringhaus, Measurements of ambipolar Seebeck coefficients in high-mobility diketopyrrolopyrrole donor − acceptor copolymers, Adv. Electron. Mater. **3,** 1700225 (2017).

[48] K. P. Ong, X. Fan, A. Subedi, M. B. Sullivan, and D. J. Singh, Transparent conducting properties of $SrSnO_3$ and $ZnSnO_3$, APL Mater. **3,** 062505 (2015).

[49] T. Kamiya, K. Nomura, and H. Hosono, Present status of amorphous $In − Ga − Zn − O$ thin-film transistors, Sci. Technol. Adv. Mater. **11,** 044305 (2010).

[50] T. Ha, P. Sonar, and A. Dodabalapur, Charge transport study of high mobility polymer thin-film transistors based on thiophene substituted diketopyrrolopyrrole copolymers, Phys. Chem. Chem. Phys. **15,** 9735 (2013).

[51] Y. Li, P. Sonar, L. Murphy, and W. Hong, High mobility diketopyrrolopyrrole (DPP)-based organic semiconductor materials for organic thin film transistors and photovoltaics, Energy Environ. Sci. **6,** 1684 (2013).

[52] B. Y. Li, S. P. Singh, and P. Sonar, A high mobility P-type DPP-thieno [3,2- b] thiophene copolymer for organic thin-film transistors, Adv. Mater. **22,** 4862 (2010).

[53] H. Yun, H. H. Choi, S. Kwon, Y. Kim, and K. Cho, Conformation-insensitive ambipolar charge transport in a diketopyrrolopyrrole-based co-polymer containing acetylene linkages, Chem. Mater. **26,** 3928 (2014).

[54] J. Rivnay, R. Noriega, J. E. Northrup, R. J. Kline, M. F. Toney, and A. Salleo, Structural origin of gap states in semicrystalline polymers and the implications for charge transport, Phys. Rev. B **83,** 121306(R) (2011).

[55] I. N. Hulea, S. Fratini, H. Xie, C. L. Mulder, N. N. Iossad, G. Rastelli, S. Ciuchi, and A. F. Morpurgo, Tunable Fröhlich polarons in organic single-crystal transistors, Nat. Mater. **5,** 982 (2006).

[56] S. Kim and A. Dodabalapur, polymer field-effect transistors Polarization effects from the ambient and the gate dielectric on charge transport in polymer field-effect transistors, Appl. Phys. Lett. **110,** 243302 (2017).

[57] T. W. Kelley and C. D. Frisbie, Gate voltage dependent resistance of a single organic semiconductor grain boundary, J. Phys. Chem. B **105,** 4538 (2001).

[58] S. Wo, R. L. Headrick, and J. E. Anthony, Fabrication and characterization of controllable grain boundary arrays in solution-processed small molecule organic semiconductor films, J. Appl. Phys. **111,** 073716 (2012).

[59] T. J. Ha, P. Sonar, and A. Dodabalapur, Improved performance in diketopyrrolopyrrole-based transistors with bilayer gate dielectrics, ACS Appl. Mater. Interfaces **6,** 3170 (2014).

[60] See Supplemental Material at http://link.aps.org/supplemental/10.1103/PhysRevApplied.11.064039 for the fitting of a polymer device with mobility greater than 10 cm^2/(Vs).

[61] T. Ando, A. B. Fowler, and F. Stern, Electronic properties of two-dimensional systems, Rev. Mod. Phys. **54,** 437 (1982).

[62] R. A. Street, J. E. Northrup, and A. Salleo, Transport in polycrystalline polymer thin-film transistors, Phys. Rev. B **71,** 165202 (2005).

[63] W. L. Kalb and B. Batlogg, Calculating the trap density of states in organic field-effect transistors from experiment: A comparison of different methods, Phys. Rev. B **81,** 035327 (2010).

[64] S. Lee, A. Nathan, Y. Ye, Y. Guo, and J. Robertson, Localized tail states and electron mobility in amorphous ZnON thin film transistors, Sci. Rep. **5,** 13467 (2015).

[65] G. Horowitz, R. Hajlaoui, and P. Delannoy, Temperature dependence of the field-effect mobility of sexithiophene. determination of the density of traps, J. Phys. III France **5,** 355 913 (1995).